Claremont Colleges
Scholarship @ Claremont

Pomona Senior Theses

Pomona Student Scholarship

2007

The Effects of Spin-Orbit Coupling on Gravitational Wave Uncertainties

C. L. Wainwright
Pomona College

Recommended Citation

The Effects of Spin-Orbit Coupling on Gravitational Wave Uncertainties

C. L. Wainwright

Advisor: T. A. Moore

April 27, 2007

Pomona College

Acknowledgments

First and foremost, I would like to thank my advisor Thomas A. Moore for his invaluable help and guidance over the past eight months as I researched this project. Without his weekly meetings, this thesis would not have been half of what it is now. I would also like to thank Rachel Paterno-Mahler for the many fine comments on a draft that I gave her.

Finally, I would like to thank my parents for their love and support throughout my four years at college, and my sister Adelaide for her wise words and the encouragement that she has given me during the stress of senior year.

Contents

ABSTRACT

I present a discussion on the expected uncertainty of orbital parameters of binary stars as measured by the space-based gravitational wave observatory LISA (Laser Interferometer Space Antenna). Specifically, I discuss how the inclusion of spin in the model of the binary stars affects the uncertainty. I found the uncertainties by calculating the received gravitational wave from a binary pair and then performing a linear least-squares parameter estimation. I performed analysis on the case of a 1500 solar mass black hole that is 20 years from coalescing with a 1000 solar mass black hole, both of which are 50×10^6 light years away. My results show that the inclusion of spin has a negligible effect upon the angular resolution of LISA, but it can increase the accuracy in the mass and distance measurements by factors of 15 and 65, respectively.

CHAPTER 1

Introduction

Since the dawn of mankind, people have looked towards the heavens and observed the motions of the celestial bodies. Until relatively recently, astronomers saw only the visible light that shone upon the Earth. Although it is a powerful tool, visible light comprises a tiny fraction of the total electromagnetic spectrum. When scientists invented new types of astronomy, such as X-ray astronomy and radio astronomy, the amount of available information grew enormously. We are currently on the cusp of another observational breakthrough. We can now view nearly the entire electromagnetic spectrum, but we are limited by the spectrum itself.

In 1915, Albert Einstein published his famous formulation of general relativity. This theory predicts, among other things, that an entirely new type of radiation permeates space: gravitational radiation. As of this writing, no gravitational radiation has been detected. However, several gravitational wave observatories are currently in operation, and several more are being constructed or are in the planning stages of development.

Here, I am interested in one such planned observatory: the Laser Interferometer Space Antenna (or LISA). My goal is to determine the certainty with which LISA can measure the orbital parameters of a specific class of astrophysical objects, which are binary systems of massive spinning bodies. In the following sections, I will give a more thorough introduction to the nature of gravitational waves, the motivation for and expectations of LISA, and the motivation for this particular experiment. I will then delve into the nature of binary orbits and describe the method that I use to achieve my goal. Finally, I will produce and analyze numerical results.

1. Gravitational Radiation

Gravitational radiation is, in many ways, very similar to electromagnetic radiation. Both propagate across space at the speed of light, both are transverse waves, and both are fundamentally caused by accelerating bits of matter. However, the waves themselves propagate in very different manners.

In classical electromagnetic radiation, oscillating electric and magnetic fields travel through empty space. The electric field is always aligned perpendicular to the

magnetic field, and both fields are perpendicular to the direction of travel. Therefore, electromagnetic radiation can be described as a superposition of two different polarizations: vertical and horizontal. These polarizations correspond to the position of the electric field.

In the theory of general relativity, gravitational radiation does not travel through empty space, but is instead embedded inside of empty space. The distinction between these two phrases is subtle, but very important. Gravitational radiation does not create fields that oscillate on top of space-time. Instead, gravitational radiation oscillates the structure of space-time itself. It squeezes space in one direction and stretches it in the other. If two small masses are exposed to a gravitational wave, then the masses will periodically come closer together and grow farther apart. However, this is not due to any forces that act upon the masses, and the masses themselves do not feel any acceleration. Instead, the space between the masses successively grows and shrinks as the wave passes by.

Like electromagnetic radiation, gravitational radiation has two possible polarizations that correspond to the orientation of its oscillations. Plus polarization (+) corresponds to a wave that stretches and squeezes space both vertically and horizontally with respect to a given viewpoint, and perpendicular to the direction of the wave's travel. Cross polarization (×) corresponds to a wave that stretches and squeezes space diagonally with respect to the same viewpoint. Of course, one may simply rotate one's frame of reference to change a plus polarization into a cross, and a cross polarization into a plus. Any gravitational wave can be decomposed into these two polarizations so that they can be treated independently.

The actual amount by which gravitational radiation displaces objects is incredibly small. The strongest gravitational waves that pass through the earth have an amplitude on the order of 10^{-21} (Hartle, 2002, pg. 335). This signifies a displacement of 10^{-21} meters for every 1 meter of distance between two objects. To put this into perspective, if such a wave were to strike the solar system, the change in the distance between the earth and the sun would be about equal to the diameter of a single atom. If gravitational wave observatories hope to detect any radiation, then they must be able to measure changes in distance that are much smaller than this.

2. Observing Gravitational Waves

The first indirect confirmation of gravitational radiation came in 1974 when Russell A. Hulse and Joseph Taylor Jr. discovered a peculiar type of astronomical object known as a binary pulsar (Karttunen et al., 2003, pg. 281). A pulsar is a neutron star that emits very bright radio pulses in regularly spaced time intervals, while a binary pulsar is a pulsar that happens to orbit some other compact astrophysical object. As a pulsar orbits about its companion, its motion relative to the earth causes its

signal to become Doppler shifted. By carefully measuring the Doppler shift, one can very accurately measure a binary pulsar's orbital period. Hulse and Taylor observed that the period of their pulsar gradually decreased. In Newtonian mechanics, this situation ought to be impossible. In the absence of external forces, the system's energy and total angular momentum should be conserved. However, in general relativity this is not the case. As the two bodies circle about each other, they create periodic distortions in the curvature of space. These distortions radiate outwards in the form of gravitational waves, carrying both energy and angular momentum with them. Hulse and Taylor found that the observed decay of their pulsar's period was identical to the decay of angular momentum that is predicted by general relativity. Thus, they found the first evidence of gravitational radiation.

For many years people have tried to support Hulse and Taylor's findings with direct observations of gravitational waves. Attempts to measure gravitational radiation started in the 1960's when Joseph Weber designed a large 'bar' apparatus that was meant to resonate when gravitational waves passed through it (Shawhan, 2004). More recent attempts make use of laser interferometry, and include large scale projects like LIGO[1] (Laser Interferometer Gravitational-wave Observatory) in the U.S. and VIRGO[2] in Italy. The foundation of these two projects is the Michelson interferometer. This device consists of a laser beam that is split, sent down two long arms, reflected off of floating mirrors, and then recombined to form an interference pattern. If the length of either arm changes, as measured by the distance to the mirrors, then the interference pattern will shift. This allows one to very accurately measure small changes in the positions of the mirrors, potentially caused by gravitational radiation.

To date, no one has directly measured a gravitational wave. All ground-based detectors must cope with significant amounts of noise, which makes the detection very difficult. This noise includes seismic noise, thermal noise, and photon shot noise. At frequencies below ~ 10 Hz, seismic noise becomes enormous, making low frequency wave detection nearly impossible (Shawhan, 2004). Unfortunately, the most predictable gravitational waves lie in this frequency. As mentioned above, binary star systems steadily emit gravitational radiation as their orbits decay. For a single binary, the frequency of the radiation is simply twice the binary's orbital frequency. Therefore, the gravitational radiation will not reach frequencies of 10 Hz and above until late in the binary's evolution, just before the two bodies coalesce. Events like this are fairly rare, and we might have to wait a considerable amount of time before we get a chance to observe one.

----

[1]see `http://www.ligo.caltech.edu/`
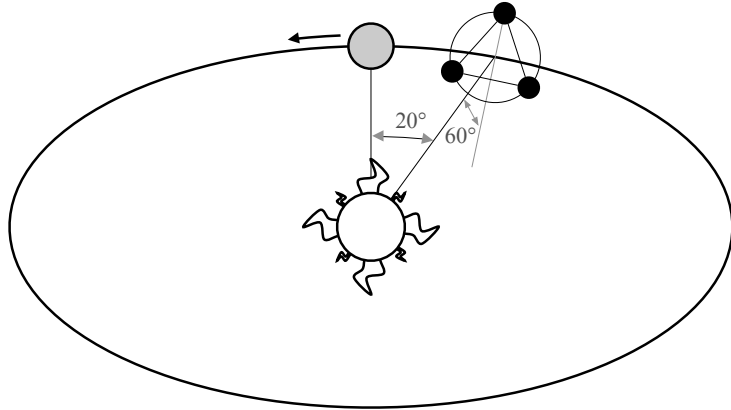[2]see `http://wwwcascina.virgo.infn.it/`

Figure 1.1: Each of the three spacecraft that comprise LISA independently orbit the sun. The orbits are such that the spacecraft form a stable equilateral triangle with sides of 5×10^6 km. The plane of this triangle is always inclined 60° away from the sun-earth orbital plane, and it trails about 20° behind the orbit of the earth.

We can avoid this problem by using LISA. LISA, the Laser Interferometer Space Antenna, is a space-based gravitational wave observatory that will orbit the Sun, trailing roughly 20° behind the earth (see figure 1.1) (Danzmann and Rüdiger, 2003). It has a planned launch date of 2015. LISA will consist of three identical spacecraft positioned five million kilometers apart, forming an equilateral triangle. Each spacecraft will point laser beams towards the other two spacecraft, which will then return laser beams that are in phase with the received light. Together, the three spacecraft will act as two giant independent Michelson interferometers. Since LISA resides in space, it is not affected by any of the seismic noise that bothers its terrestrial counterparts. It must account for other sources of noise, such as the effects of solar wind and the drift of the spacecraft, but these sources should be very small when compared to seismic noise. Therefore, LISA will be able to detect much lower frequencies of radiation than those detected by projects such as LIGO and VIRGO. In this way, LISA will complement the terrestrial observatories. Ground-based observatories should be able to measure high frequency radiation ($\gtrsim 10$ Hz) that results from violent astrophysical events, whereas LISA will excel at measuring a large range of lower frequency radiation ($\sim 1.0 - 0.0001$ Hz).

There are several different astrophysical objects that we hope to observe with LISA. There should be a large number of low-frequency, nearby binary systems that produce a detectable amount of gravitational radiation. Some of these systems are binary pulsars that astronomers have already observed with conventional telescopes. These observations will be powerful tools when calibrating the data retrieved from

LISA. Also, since the gravitational waveform that is emitted by binary systems is easily calculated from theory, data from these systems will be an excellent test of general relativity itself. Furthermore, by measuring the distribution of galactic binary systems, one may discover interesting facts about stellar evolution. Of course, LISA should be able to see not only small binaries that happen to be nearby, but also very large binaries that are very far away. For example, when two galaxies with super-massive central black holes collide, the black holes will come together due to dynamical friction[3] and form a binary pair. Another potential source of detectable gravitational radiation is the cosmic gravitational background radiation left over from the very early universe. Undoubtedly, a detection from any of these sources will produce a wealth of new information about general relativity and the objects themselves.

3. In Search of Uncertainty

I am interested in the gravitational radiation that LISA may detect from binary systems. Each binary produces a unique gravitational waveform that one can predict from a theoretical model of the binary itself. For a simple binary system in which the bodies may be approximated as non-spinning point particles, the binary and its waveform can be uniquely determined by nine parameters. Three of these correspond to the binary's orbital characteristics (the masses of the two bodies and the distance between them), three correspond to its orientation and its initial phase, and three correspond to its position in the sky and distance from the earth. In order to learn anything about the binaries from their waveforms, we must be able to measure each of these parameters as accurately as possible. Of critical importance are the positional parameters. If LISA can accurately determine the position of the binaries, then astronomers will be able to view them with optical telescopes, thus gaining additional information about them and their environments.

With this in mind, it is very useful to study the theoretical uncertainties for each of these parameters that one may obtain by analyzing the received gravitational waveform. This will allow LISA's scientists to set goals for what they can hope to achieve, and it will put limits on the resolution of individual binary systems.

Thomas A. Moore and Ronald W. Hellings have already done extensive work in this field (see Moore and Hellings, 2002). In order to calculate the uncertainties, they use the following basic method: First, they calculate what the expected waveform ought to be. They can then calculate how the waveform varies when different

---

[3]Dynamical friction is a phenomenon that causes large masses to slow down in the midst of many smaller masses. In the case of colliding galaxies, the central black holes generally do not collide with stars, but the stars can still transfer their momenta to the black hole through gravitational interactions.

parameters change. This is done by finding the partial derivatives of the waveform with respect to each of the nine parameters. Once the derivatives are found, all they need to do is to change the waveform by an amount equal to the expected noise in LISA, and then calculate the corresponding changes in the parameters. These final changes directly correspond to the uncertainties in each of the parameters. Of course, the actual mathematics behind this can be quite complicated; a more detailed explanation is given in chapter 3. However, this is the basic idea behind the calculations. As a result of their research, they found that LISA will be able to localize major non-spinning black-hole mergers with an accuracy of roughly 10^{-4} steradians (equivalent to the area of a circle in the sky with a ~ 19 arcminute radius), which is slightly larger than the angular size of the full moon, while some high-frequency binaries may be localized to within a solid angle of 10^{-8} steradians (equivalent to a circle with a ~ 12 arcsecond radius).

My goal is to extend the work performed by Moore and Hellings to include binary systems that contain spinning bodies. The inclusion of spin has several important scientific benefits. The rotation of the bodies in a binary system has both direct and indirect effects upon its waveform. These effects should be easily discernible in cases where the objects' rotational angular momenta compose a non-negligible fraction of the system's total angular momentum. Virtually all changes in the waveform also produce changes in its derivatives, so inclusion of spin will change the uncertainties of the nine basic parameters. By adding spin to the calculations, I will change the parameter space from nine to fifteen variables. The extra six variables contain the information about the spin magnitude and direction for each of the two bodies. Since the parameter space will grow, the chances of two parameters being highly correlated will increase. Again, this could cause a potentially significant change in the original uncertainties.

Including spins in uncertainty calculations is also important because the spins themselves are physically interesting. Different types of objects (like white dwarfs, neutron stars, and black holes), have different characteristic angular momenta. By measuring the uncertainties of the spin parameters, one can determine whether or not it is possible to differentiate these sources based upon spin alone.

In order to calculate and analyze the measured uncertainties of spinning coalescing binaries, I will perform the following tasks. First, in chapter 2, I will analyze the orbits of binary systems, both with and without spin. This will provide the theoretical background that is needed to calculate the uncertainties. Next, in chapter 3, I will describe how to extend the work of Moore and Hellings to include spinning objects. I will discuss the math behind the uncertainty calculations, and I will detail the additional math required for spinning objects. Finally, I will produce and analyze numerical results in chapter 4.

CHAPTER 2

Binary Orbits and Precession

In order to understand how binary spins affect gravitational radiation and uncertainties in measurements, one must first understand how the spins affect binary orbits. This chapter will introduce the basics of binary orbits. It will start with Keplerian equations of motion and simple general relativistic effects. Section 2 will explain the phenomenon of gravitomagnetism and section 3 will utilize it to explain how binary spins cause orbital precession. I will then describe the precessional equations of motion and some of their interesting features. Finally, in section 4, I will show the results of numerical simulations of the orbits and compare them to the predictions made in section 3.

1. Orbits of Non-spinning Binary Stars

The easiest way to describe binary orbits is with simple Keplerian motion. According to Kepler's third law,

$$(2.1) \qquad \left(\frac{P}{2\pi}\right)^2 = \frac{a^3}{G(m_1 + m_2)},$$

where P is the the period of the orbit, a is the semi-major axis of the orbit (or just the radius, in the case of circular orbits), and m_1 and m_2 are the masses of the two orbiting objects. This law is generally used when describing the motion of planets about the sun, and it assumes that one of the masses is much larger than the other. For the more general case with arbitrarily large or small masses, equation 2.1 needs to be modified. If the orbit is circular, then this is easily achieved by replacing a, the semi-major axis, with r, the distance between the two objects. Therefore,

$$(2.2) \qquad \left(\frac{P}{2\pi}\right)^2 = \frac{r^3}{G(m_1 + m_2)}.$$

This equation relates the period of a binary's orbit to its total mass and orbital separation. In Newtonian mechanics, this orbit is completely stable. Two objects that are set into an orbit will remain in that orbit until some external force acts upon them. However, in general relativity this is not the case.

According to the theory of general relativity, objects emit gravitational radiation as they orbit about each other. This radiation then propagates through space at the

speed of light, stretching and squeezing bits of matter through which it happens to pass. In order to perform this work, the gravitational radiation needs to carry some energy, and this energy can only come from the orbiting objects. Therefore, a binary system will slowly lose energy to gravitational radiation. The binaries' orbits will decay to lower energy levels and the separation between the objects will decrease. The release of gravitational radiation tends to circularize the orbits (Blanchet et al., 1996), so equation 2.2 does a good job at describing their motion over small periods of time. Note that as the separation decreases, the orbital period decreases and the orbital frequency increases. One can easily show that the orbital velocities go as $v \propto r^{-1/2}$, so the binaries move faster as the orbit decays. This is the basic picture of the orbital evolution of binary systems. Gravitational radiation will circularize the orbit and cause it to decay and spiral inwards, which in turn causes the orbital frequency and velocity to increase. Eventually, the two objects will coalesce, likely resulting in the creation of a black hole.

This is how binary systems evolve when neither of the orbiting objects spin. When the objects do spin, the orbital motion is complicated by precession of the orbital plane. To understand this effect, one must first learn about the phenomenon of gravitomagnetism.

2. Gravitomagnetism

Gravitomagnetism is a way of describing motion in relativistic space-time in which mass is analogous to electric charge. For the two body problem, the analogy is fairly simple. We can treat one body as if its mass is a positive charge and treat the other body as if its mass is a negative charge. In this model the two masses will attract each other because of their different charges. This is nothing new, and it adds nothing to the old Newtonian model of gravitational attraction. The real power of this analogy can be seen when one of the masses is spinning. In electromagnetism, a spinning ball of charge creates a magnetic field (figure 2.1a). This magnetic field interacts with moving charges, such that charges moving directly towards the spinning charge get deflected away (figure 2.1b). The analogous result in gravitomagnetism is that spinning masses deflect the trajectories of incoming masses. This result is not predicted by Newtonian gravitation, but it is predicted by general relativity. For an in depth discussion on the physics behind this phenomenon, see Appendix A.

The gravitomagnetic analogy is not merely qualitative. Starting from the basic equations of general relativity and working in the weak-field limit, one can derive a set of laws that are exactly analogous to Maxwell's equations of electromagnetism
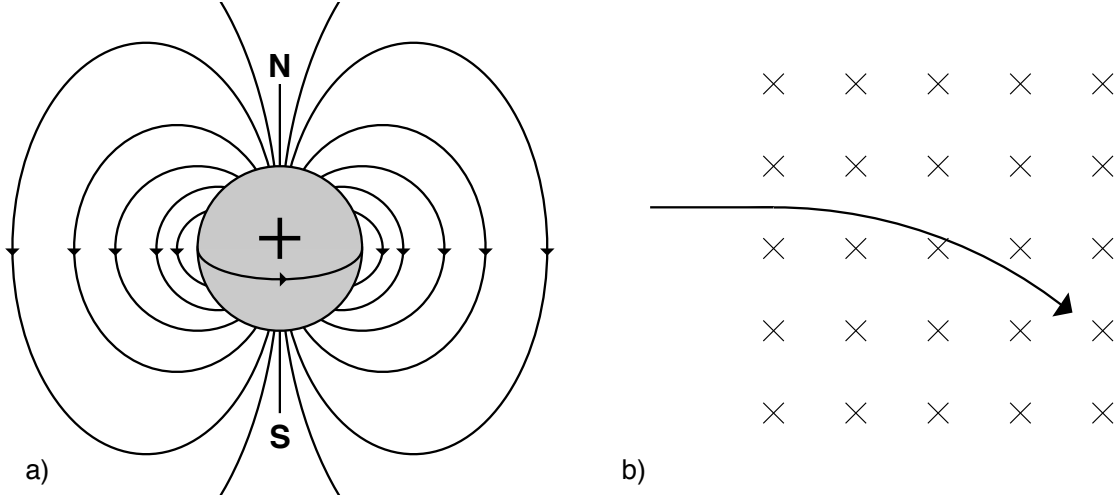
Figure 2.1: a) A spinning ball of charge creates a magnetic field, much like an ordinary magnet. For a positive charge spinning to the right, the field will point up out of the charge's top. b) A moving charge in a magnetic field gets deflected in a direction that is perpendicular to both the field and its own motion. In a uniform field, the charge will move in a circle.

(Mashhoon et al., 2001). These are

$$(2.3a) \qquad \nabla \cdot \boldsymbol{G}_E = 4\pi G\rho \qquad\qquad \nabla \times \boldsymbol{G}_E = -\frac{1}{c}\frac{\partial}{\partial t}\boldsymbol{G}_B$$

$$(2.3b) \qquad \nabla \cdot \boldsymbol{G}_B = 0 \qquad\qquad \nabla \times \boldsymbol{G}_B = +\frac{1}{c}\frac{\partial}{\partial t}\boldsymbol{G}_E + \frac{4\pi}{c}G\boldsymbol{J},$$

where $\boldsymbol{G}_E$ is the gravitoelectric field, $\boldsymbol{G}_B$ is the gravitomagnetic field, G is the gravitational constant, ρ is the local mass density, and $\boldsymbol{J}$ is the local mass current density.[1] The only differences between these equations and Maxwell's equations are the replacement of charge with mass and a change in coefficients. One can also derive an analogy to the Lorentz force equation, where the total gravito-electromagnetic force on a small object of mass m and velocity $\boldsymbol{v}$ is given by

$$(2.4) \qquad\qquad \boldsymbol{F}_G = -m\left(\boldsymbol{G}_E + \frac{\boldsymbol{v}}{c} \times 2\boldsymbol{G}_B\right).$$

This differs from the Lorentz force equation for electrodynamics in two important respects. First, there is now a negative sign in front of the equation. This is because positive masses attract each other, whereas like charges repel each other.[2] Second,

---

[1]Note that bold font denotes vector quantities.

[2]We could have just as easily defined the fields in equations 2.3 to be negative, and left equation 2.4 to be positive. For this paper, I am choosing the force to be negative such that a moving
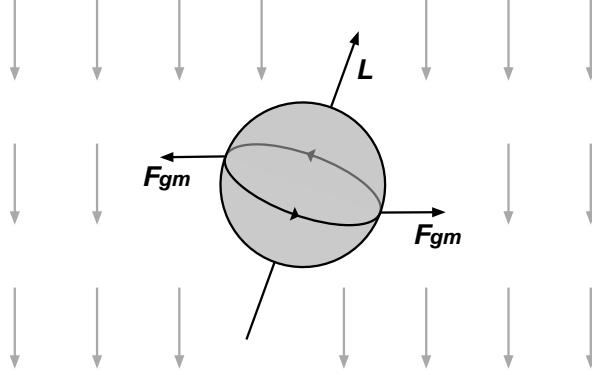
Figure 2.2: A spinning massive object experiences a torque that tries to anti-align its angular momentum with the gravitomagnetic field, represented here as the grey downward arrows. The right side of the object moves with a velocity that is directed into the page. This creates a force, via equation 2.4, that pulls the right side of the object to the right. Similarly, the left side of the object pulls to the left. Therefore, the net torque points directly out of the page.

there is now a coefficient of 2 in front of $\boldsymbol{G}_B$. This is an odd result that is due to the spin-2 nature of the gravitational field[3] (Mashhoon et al., 2001).

Now that we have this powerful analogy, we can use it to provide a qualitative explanation of the orbits of spinning binary stars.

3. Precessional Equations of Motion

We can start to analyze the equations of motion by looking at the behavior of a single rotating mass in a uniform gravitomagnetic field. In such a field, a rotating mass will experience a torque that tries to anti-align the object's spin axis and angular momentum with the surrounding field. This can be seen in figure 2.2. The individual forces acting upon the object are governed by equation 2.4, so they are proportional to the total mass, the speed at which it is spinning (which equals the angular velocity ω times the radius at which the force is acting), and the strength of the gravitomagnetic field. The individual torques, defined as $\boldsymbol{\tau} = \boldsymbol{r} \times \boldsymbol{F}$, are proportional to the magnitude of the forces and the radius of the object. Therefore, the net torque has the following relation:

$$\boldsymbol{\tau}_{gm} \propto mr(r\boldsymbol{\omega}) \times \boldsymbol{G}_B.$$

---

mass and a moving positive charge create gravitomagnetic and electromagnetic fields that point in the same direction.

[3]The spin of the gravitational field describes the fundamental nature of gravity, not the macroscopic properties of objects in the field. In contrast, the electromagnetic field and its force carrying the particle, the photon, are both spin-1.

Or, more succinctly,

$$(2.5) \qquad\qquad \boldsymbol{\tau}_{gm} \propto \boldsymbol{L} \times \boldsymbol{G}_B,$$

where $\boldsymbol{L} = I\boldsymbol{\omega}$ is the object's angular momentum, and I is its moment of inertia. For a sphere $I = \frac{2}{5}mr^2$, although this varies with different shapes. By taking advantage of the relation $\boldsymbol{\tau} = \dot{\boldsymbol{L}}$,[4] one can rewrite equation 2.5 as

$$(2.6) \qquad\qquad \dot{\boldsymbol{L}} \propto \boldsymbol{L} \times \boldsymbol{G}_B.$$

This equation shows that the object's angular momentum drifts with time while its magnitude stays constant. The drift traces out a circle in momentum space that repeats with a period of $T \propto \frac{2\pi}{|\boldsymbol{G}_B|}$. Therefore, a spinning object's angular momentum will precess about its surrounding gravitomagnetic field with a constant precessional frequency of $f \propto \frac{|\boldsymbol{G}_B|}{2\pi}$.

There are two sources of gravitomagnetic fields in a binary system: the individual spinning objects and the orbit of the binary itself. Each of the objects creates a small gravitomagnetic dipole (see figure 2.1) whose strength decreases as one over the cube of the distance from the object's center. The movement of the objects through space also create gravitomagnetic fields, giving rise to a total orbital gravitomagnetic field. This field is related to the total orbital angular momentum of the system and to the masses of the individual bodies in a somewhat complicated way. Each object independently precesses in the fields of its neighbor and its orbit. The orbital angular momentum precesses in a similar manner to that of the individual objects; it precesses about each of the gravitomagnetic fields created by the spinning masses.

With this in mind, we can now write down the precessional equations of motion. Let m_1 and m_2 be the masses of the objects, $\boldsymbol{S}_1$ and $\boldsymbol{S}_2$ be the spin angular momenta of the objects, and $\boldsymbol{L}$ be the orbital angular momentum of the whole system. The equations of precession are then

$$(2.7a) \qquad \dot{\boldsymbol{S}}_1 = \frac{G}{2r^3c^2}\left[(\boldsymbol{L}\times\boldsymbol{S}_1)\left(4+3\frac{m_2}{m_1}\right)+\boldsymbol{S}_2\times\boldsymbol{S}_1-3\left(\hat{\boldsymbol{L}}\cdot\boldsymbol{S}_2\right)\hat{\boldsymbol{L}}\times\boldsymbol{S}_1\right]$$

$$(2.7b) \qquad \dot{\boldsymbol{S}}_2 = \frac{G}{2r^3c^2}\left[(\boldsymbol{L}\times\boldsymbol{S}_2)\left(4+3\frac{m_1}{m_2}\right)+\boldsymbol{S}_1\times\boldsymbol{S}_2-3\left(\hat{\boldsymbol{L}}\cdot\boldsymbol{S}_1\right)\hat{\boldsymbol{L}}\times\boldsymbol{S}_2\right]$$

$$(2.7c) \qquad \begin{aligned} \dot{\boldsymbol{L}} = \frac{G}{2r^3c^2}&\left\{\left[\left(4+3\frac{m_2}{m_1}\right)\boldsymbol{S}_1+\left(4+3\frac{m_1}{m_2}\right)\boldsymbol{S}_2\right]\times\boldsymbol{L}\right. \\ &\left.-3\left[\left(\hat{\boldsymbol{L}}\cdot\boldsymbol{S}_2\right)\boldsymbol{S}_1+\left(\hat{\boldsymbol{L}}\cdot\boldsymbol{S}_1\right)\boldsymbol{S}_2\right]\times\hat{\boldsymbol{L}}\right\}, \end{aligned}$$

where $\hat{\boldsymbol{L}}$ is a unit vector pointing in the same direction as $\boldsymbol{L}$ (Kidder, 1995). Even though these equations look rather complicated, they are actually simplified versions

---

[4]Here I use the common dot notation to represent a coordinate-time derivative.

of even more general equations of motion. Generally, the orbital angular momentum can be decomposed into several different parts that appear differently on the left and right sides of equation 2.7c. These include a component that is due to purely Newtonian mechanics, as well as some components that are due to general relativistic effects such as spin-orbit coupling (see Kidder 1995 for a full list of these effects). However, the general relativistic effects average to zero over one full orbit, so as long as the precessional frequency is much larger than the orbital frequency we can safely assume that the Newtonian component acts as a good approximation to the total angular momentum. Otherwise, the orbital precession would show a slight wobble for each orbital period.

Let us now see how well our gravitomagnetic model describes equations 2.7. For each of the two spin equations (equations 2.7a and 2.7b) there are three terms. Note that each term has the r^{-3} dependence that we predicted from the gravitomagnetic dipole model of spinning masses. The first term shows how the direction of the spin precesses about the field created by the orbital angular momentum. Its coefficient is a function of the mass of the two objects, and the smaller mass experiences a larger torque than its neighbor. This is simply because the larger mass creates a larger gravitomagnetic field as it orbits, so it exerts a larger torque. The second term shows how the first mass precesses about the second mass's spin vector. Since the gravitomagnetic field is directly proportional to the magnitude of the spin angular momentum, this second term only involves a single factor of S_2. The third term is somewhat complicated, and it is not immediately obvious how it falls out of equation 2.6. It is easiest to think of it as a correction to the second term. The field of a dipole is axially symmetric, not radially symmetric, so the torque exerted by one object upon another will change as the first object tips in any given direction. The last term takes this tip into account.

Equation 2.7c only has two terms. The first term is analogous to the first terms in equations 2.7a and 2.7b. It describes how the orbital angular momentum precesses about the spins, while the second term is analogous to the third terms in the preceding equations. In sum, the orbital angular momentum vector will precess about the two spin vectors because of the gravitomagnetic fields that they create, and the spin vectors will likewise precess about the orbital angular momentum vector and each other.

Equations 2.7 describe a system of differential equations with three 3-dimensional vectors, or nine different variables. However, there are several conserved quantities in this system, so we need not trouble ourselves with all nine of them. As noted above, the vectors themselves have constant magnitudes since their time derivatives are perpendicular to their positions. Also, since the system is isolated, the total

angular momentum is conserved; that is,

$$(2.8) \qquad \boldsymbol{\dot{J}} \equiv \boldsymbol{\dot{L}} + \boldsymbol{\dot{S}}_1 + \boldsymbol{\dot{S}}_2 = 0,$$

or equivalently,

$$(2.9) \qquad \boldsymbol{\dot{L}} = -\left(\boldsymbol{\dot{S}}_1 + \boldsymbol{\dot{S}}_2\right).$$

One can easily check that this relationship is true in equations 2.7. We can then rewrite the precessional equations in terms of $\boldsymbol{J}$ and reduce the number of variable vectors from three to two. Also, we can now characterize equation 2.7c as the much simpler and more intuitive equation of conservation of angular momentum seen in equation 2.9.

If only one mass is spinning, then equations 2.7 reduce to

$$(2.10a) \qquad \boldsymbol{\dot{S}}_1 = \frac{G}{2r^3c^2}\left(4 + 3\frac{m_2}{m_1}\right)\boldsymbol{J} \times \boldsymbol{S}_1$$

$$(2.10b) \qquad \boldsymbol{\dot{L}} = \frac{G}{2r^3c^2}\left(4 + 3\frac{m_2}{m_1}\right)\boldsymbol{J} \times \boldsymbol{L}.$$

Both the spin vector and the orbital angular momentum vector will precess circularly about the total angular momentum in the same direction, and the orbital plane of the two objects will shift as the orbital angular momentum precesses. One can easily show that the frequency of the precession is

$$(2.11) \qquad f = \frac{G}{4\pi r^3c^2}\left(4 + 3\frac{m_2}{m_1}\right)J,$$

where J is the magnitude of the total angular momentum. This is the simplest possible type of precession.

If both masses are spinning, the precession of $\boldsymbol{L}$ is much more complicated. Equations 2.7 cannot be reduced, and the inclusion of $\boldsymbol{J}$ only makes them more complicated. The orbital angular momentum still precesses about the total angular momentum, but it also precesses about the individual spins with different characteristic frequencies. Since the spins are not constant, the spin precession causes the orbital angular momentum to wobble outside of a simple circular precession.

So far, the discussion of precession has ignored the effects of gravitational radiation. I have implicitly assumed that the gravitational radiation is small enough that the orbital frequency is approximately constant and that the binary orbit does not decay. However, late in a binary's life this assumption becomes invalid. The r in equations 2.7 will no longer be constant, and equation 2.7c will contain an extra term that describes how the gravitational radiation carries away angular momentum. These effects will cause the precession to speed up and the wobble of the orbital plane

to increase in size (Kidder, 1995). For simplicity, I will ignore these effects in the rest of this thesis and focus only on binary systems that are far from coalescence.

4. Precession Simulations

In order to test the predictions made in the previous section, I wrote and ran numerical simulations of binary systems. I wrote the simulation in the REALbasic programming environment, and I used a fourth order Runge-Kutta algorithm to solve the relevant differential equations (equations 2.7). I will present data for two different cases: one where one object is spinning, and one where both objects are spinning. In each case, the objects orbit with a period of 1000 seconds. The first object has a mass of 10^6 solar masses, while the second object has a mass of 5×10^5 solar masses. By Kepler's third law (equation 2.2), the orbital separation is 17.1 million kilometers. These values place the binary in a regime where the precessional frequency is comparable to the orbital frequency, and where the orbital frequency changes significantly with time. Since this violates the assumptions implicit in equations 2.7 and 2.8, these particular cases do not do a good job at simulating actual astrophysical objects. However, they clearly show the precession of the orbital plane since the orbital angular momentum is of the same order of magnitude as the spin angular momenta, so they are useful for the current discussion. Other cases—where $|\boldsymbol{L}| \gg |\boldsymbol{S}|$ and the assumptions of low precessional frequency and constant orbital frequency are not violated—will have similar qualitative features to the cases discussed here, but their precession will not be as easily noticeable. In all cases the coordinate system is oriented such that the z-axis coincides with the constant total angular momentum $\boldsymbol{J}$.

For the first case, where only one object is spinning, I modeled the situation by setting the larger mass's spin vector to coincide with the x-axis. I treated the object as a maximally spinning black hole with $|\boldsymbol{S}| = Gm^2/c$ (see chapter 3.1). This causes the orbital angular momentum to be tipped $\sim 45.9°$ away from the z-axis in the $-x$ direction so that the total angular momentum remains on the z-axis. The precession here is very simple, as predicted by equations 2.10. The orbital angular momentum vector precesses about the z-axis in a perfect counter-clockwise circle (as viewed from above the xy-plane) with a constant precessional frequency of 0.0549 mHz. It maintains its constant zenith angle of $45.9°$. This is exactly the behavior that was expected in section 3, and the observed precessional frequency exactly matches the theoretical value given by equation 2.11.

In the second case, I treated both objects as maximally spinning black holes. The larger object's spin vector initially points in the $+x$ direction, while the smaller object initially points in the $+y$ direction. The orbital angular momentum is then tilted $\sim 47.8°$ away from the z-axis. Since we now have both objects spinning, we
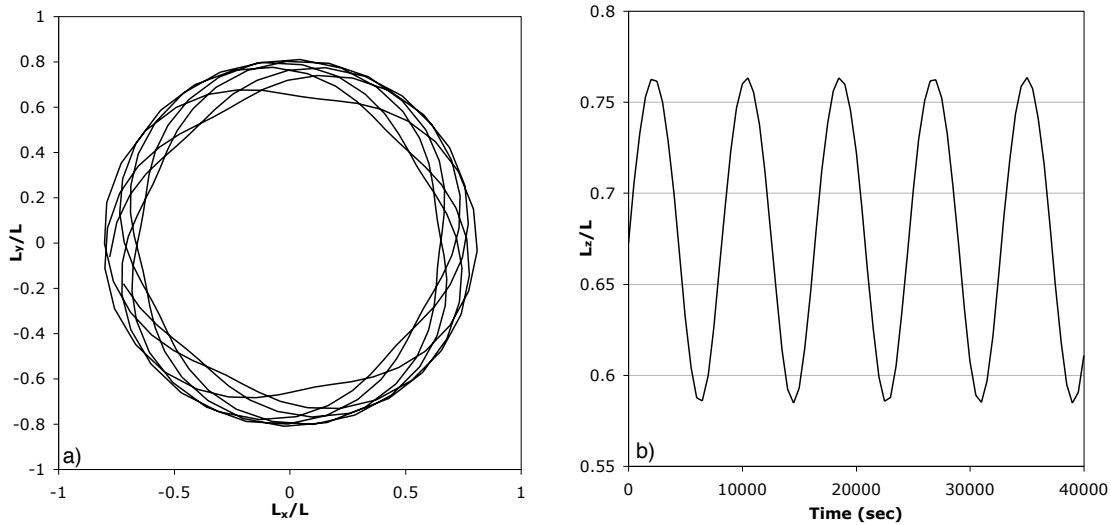
Figure 2.3: a) Projection of the orbital angular momentum onto the xy-plane for the case of two spinning bodies. The graph shows 7 full counter-clockwise precessions over a time of 128,000 seconds. b) The z component of the orbital angular momentum as a function of time. Note that the zenith angle can be expressed as $\theta = \cos^{-1}(L_z/L)$.

must use the full precessional equations. At any given moment of time, the orbital angular momentum independently precesses about both of the spin vectors, and the frequency of this precession depends upon the orientation of the spin vectors with respect to the orbital plane. On average, the orbital angular momentum still precesses about the z-axis, but it no longer precesses in a neat circle. Instead, it sways back and forth about a zenith angle of $\sim 47.0°$ as its interaction with the spin vectors force it to move up and down (figure 2.3b). This creates the spirograph pattern seen in figure 2.3a.

The frequency of precession is no longer a simple value to calculate. This is because the precession of the orbital angular momentum can no longer be neatly written in terms of $\boldsymbol{J}$, and because it now precesses with several different characteristic frequencies. In order to determine what these frequencies are, I performed a fast Fourier transform on the orbital angular momentum's three components. Figure 2.4 shows the relative strengths of the different precessional frequencies for the x and the z components. The x component shows the frequencies at which it precesses about $\boldsymbol{J}$, while the z component shows how it oscillates about the zenith angle of $47.0°$.

Interestingly, the primary precessional frequency (~ 0.055 mHz) is very close to the precessional frequency for the case of one spinning object. It is as if the orbital
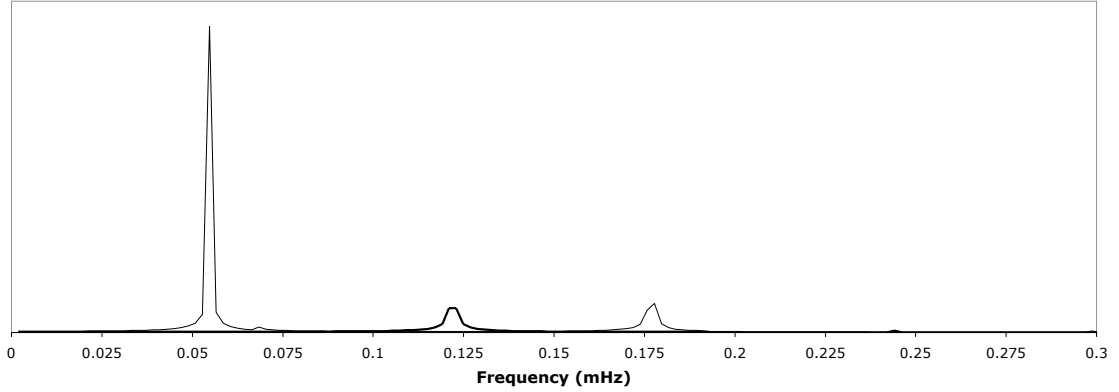
Figure 2.4: This graph shows the orbital angular momentum transformed into frequency space for the case of two spinning bodies. The thick line represents the relative frequencies in the z component, while the thin line represents the relative frequencies in the x component. The z component has a major peak at 0.122 mHz and a minor peak at 0.244 mHz. The x component has major peaks at 0.055 mHz and 0.177 mHz, and a minor peak at 0.068 mHz.

angular momentum precesses about the spin of the larger object independently of the spin of the smaller object. However, it does not appear to precess about the smaller object independently of the larger object. If only the small object were spinning, then by equation 2.10 we would expect the precessional frequency to be roughly 0.14 mHz, but this frequency is not seen when both objects are spinning.

There is no obvious way to explain the other major frequency peaks in either of the two momentum components independently. However, there is an important connection between the two major peaks in the x component and the single major peak in the z component: the difference in the frequencies in the x component equals the primary frequency in the z component. This can be understood as follows: the orbital angular momentum is constant, so any increase in L_x and L_y will be accompanied by a decrease in L_z. L_x and L_y oscillate together[5] at the two different frequencies seen in the x component of figure 2.4. When these frequencies are in phase, L_x and L_y grow large and L_z grows small. The reverse happens when they are out of phase. Because of the properties of periodic functions, the frequencies pulse in and out of phase at a frequency that is precisely equal to their difference. This is why the frequency of the z component is equal to the difference of the two frequencies in the x component.

---

[5]Since the system is axially symmetric, L_x and L_y must always oscillate at exactly the same frequencies. At any given moment, the two components will be exactly 90° out of phase with respect to each other.

The complicated orbital precession of two spinning objects creates a unique frequency signature, as seen in figure 2.4. Scientists working on LISA ought to be able to detect this signature and use it to gain insight into the orbits of binary stars.

Finding Uncertainties

The main goal of my research is to determine how the spin-orbit precession of binary stars affects the certainty with which LISA can measure their orbital parameters. This chapter details the strategy that I used to achieve this goal. First, in section 1, I list all of the measurable orbital parameters for a binary system. Then, in section 2, I describe the statistical methods that Moore and Hellings used to determine the uncertainties of the orbital parameters of non-spinning binary stars. Finally, I show how to extend these methods to spinning binary stars in section 3.

1. Orbital Parameters

There are exactly nine parameters that describe the orbits of non-spinning binary stars. The first three parameters describe the location of the binary with the use of a spherical coordinate system centered on the sun. There is the zenith angle Θ, defined so that an angle of $90°$ places the binary on the ecliptic plane;[1] the azimuth angle Φ; and the radial coordinate r.[2]

The next three parameters describe the orientation of the binary in the sky (see figure 3.1). The first of these parameters is the inclination i. The inclination is the angle between the orbital angular momentum vector and the line of sight. The next parameter is ψ. This describes the direction that the angular momentum vector points when it is projected onto a plane that is normal to the line of sight. The last positional parameter is the phase ϕ_0. Note that the phase is defined in terms of a reference angle that is determined by ψ.

The final three parameters describe the physical orbit of the binary itself. Two parameters describe the objects' masses. The total mass is given by the parameter τ, which is expressed in units of time:

$$(3.1) \qquad \tau = \frac{5G(m_1 + m_2)}{c^2}.$$

---

[1]The ecliptic plane is the plane defined by the Earth's orbit around the sun.

[2]In cosmology there are several different ways to define distance. Here, the radial coordinate is always measured as the geometric distance to the object. The geometric distance to an object is the distance that one would measure with a tape measurer at the current (comoving) coordinate time.
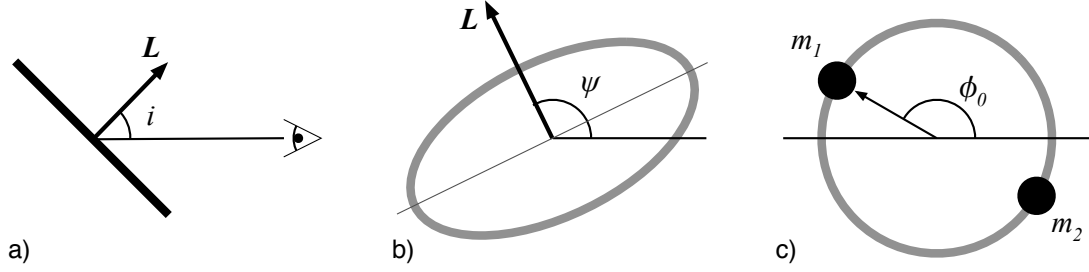
Figure 3.1: a) The inclination is defined as the angle between the orbital angular momentum $\boldsymbol{L}$ and the line of sight. b) The angle ψ is the angle between $\boldsymbol{L}$ projected onto a plane normal to the line of sight and a horizontal reference line, which is parallel to Earth's ecliptic plane. c) The phase of the orbit ϕ_0 is defined as the angle to the first object from a reference line. The reference line is defined to be the major axis of the orbit when viewed as an ellipse.

The mass difference is given by the unitless parameter δ:

$$(3.2) \qquad\qquad \delta = \frac{m_1 - m_2}{m_1 + m_2}.$$

The final parameter is the time to coalescence, t_c. Given the masses of the two objects, this last parameter effectively specifies the orbital separation and the orbital period.

In order to describe spinning binary stars we need to add six more parameters. Each star needs one parameter that defines the magnitude of its angular momentum $\boldsymbol{S}$, and two parameters that define its orientation. Let the magnitude of the spin vector be defined as

$$(3.3) \qquad\qquad |\boldsymbol{S}| \equiv \chi \frac{Gm^2}{c},$$

where χ is a unitless parameter. Theory predicts that black holes will have $\chi \leq 1$, and neutron stars will have $\chi \sim 0.7$ (Kidder, 1995). The orientation of $\boldsymbol{S}$ can easily be written in spherical coordinates with a zenith angle of θ and an azimuth angle of ϕ. An angle of $\theta = 0°$ corresponds to a spin that is parallel to the total angular momentum $\boldsymbol{J}$, and ϕ is defined such that a vector pointing from the binary to Earth will have an azimuth angle of $\phi = 180°$ (see figure 3.2).

It is also useful to introduce parameters that describe the orientation of the total angular momentum $\boldsymbol{J}$. Let us denote these parameters as i_J and ψ_J. If neither of the masses spin, then $i_J = i$ and $\psi_J = \psi$. However, if there is spin, then $\boldsymbol{J}$ and $\boldsymbol{L}$ will point in different directions and have different orientations. Since $\boldsymbol{J}$ is constant and its orientation does not change, it is easier to describe spinning binaries in terms of i_J and ψ_J than in terms of i and ψ.

This leaves us with 15 parameters in total: Θ, Φ, r, i_J, ψ_J, ϕ_0, τ, δ, t_c, χ_1, θ_1, ϕ_1, χ_2, θ_2, and ϕ_2. The next two sections will describe how to find the uncertainty in each of these parameters as measured by LISA.

2. Structure of the Original Program

At its most basic, LISA can only detect the phase changes of the lasers in the three arms that comprise its interferometer, only two of which act independently.[3] All information about gravitational radiation must be inferred from this. In the low frequency limit, the phase change is directly proportional to the amplitude of passing gravitational waves (Moore and Hellings, 2002). For a given source, this can then be written in terms of the wave's plus and cross polarizations:

$$(3.4) \qquad h(t) = F_+(t)h_+(t) + F_\times(t)h_\times(t),$$

where $h_+(t)$ and $h_\times(t)$ are the amplitudes of the plus and cross polarizations and $F_+(t)$ and $F_\times(t)$ are time-dependent beam-pattern functions. The beam-pattern functions depend on LISA's instantaneous position about the sun and the position and orientation of the binary source in the sky (parameters Θ, Φ and ψ). The amplitudes of the two polarizations depend on the distance to the source r; its inclination i; its orbital parameters τ, δ, and t_c; and the received phase of the gravitational wave. The phase primarily depends upon the initial phase of the source ϕ_0 and the evolution of the phase as the stars orbit each other, which is determined by the orbital parameters. However, the phase also changes when the gravitational radiation gets Doppler-shifted, due both to the orbiting of LISA and to cosmological redshift. Thus, the laser-phase change measured by LISA is a function of all nine original binary parameters.

In their program, T. A. Moore and R. W. Hellings find the uncertainty in the binary parameters in the following manner: first, they assume that LISA has recorded n individual observations h_i of a single gravitational wave and that someone has already found a set of parameters that approximately match these observations. Each observation will still differ from the theoretically predicted value by some amount $y_i = h_{i,observed} - h_{i,predicted}$. They then use linear least-squares parameter estimation to tweak the binary parameters such that the noise associated with each measurement is minimized. Using this method, they show that if one defines a 9×9 information matrix

$$(3.5) \qquad A_{ab} \equiv \sum_{i=1}^{n} \frac{\partial h_i}{\partial q_a} \frac{\partial h_i}{\partial q_b},$$

---

[3]The phase change in the third arm can be written as a linear combination of the other two.

where q_a and q_b can represent any of the nine different parameters, then the uncertainty σ_a in a single parameter q_a is given by

$$(3.6) \qquad\qquad\qquad \sigma_a = \sigma_y \sqrt{A_{aa}^{-1}},$$

where σ_y is the uncertainty in the observations and A^{-1} is the inverse of the information matrix A.

The computer program that finds these uncertainties can be divided into five distinct tasks, all of which are implemented in the REALbasic programming environment: input, setup, computation of the information matrix, evaluation of uncertainties, and output. In input, the user must set the 9 different parameters that define the binary system. Then, in setup, the program calculates many different constants that are useful in later steps. The heart of the program lies in the computation of the information matrix. At this point, the program enters a loop. Each step of the loop corresponds to a single observation h_i of the hypothetical gravitational wave. During each step it must compute the amplitudes of the plus and cross polarizations, the time-dependent beam-pattern functions, the phase and frequency evolution of the received wave (including Doppler shifts), and finally the derivatives that comprise the information matrix. These derivatives are calculated by a tedious application of differential calculus. Once the information matrix calculation is complete, the program simply inverts the matrix and multiplies it by the frequency dependent noise (i.e., the uncertainty σ_y) in order to calculate the uncertainties of the individual parameters. In the final task, these outputs are printed to the screen so that the user may save them for later use.

3. Addition of Spin

Including spin in the program causes a fundamental problem: the orientation of a binary's orbital plane is no longer constant, and the variables ψ and i vary with time. This problem dominated the modifications that I needed to make in the rest of the program. Before describing these modifications, it will be helpful to explain exactly how ψ and i depend upon the orientation of a binary's orbital plane and its orbital angular momentum $\boldsymbol{L}$.

There are two different coordinate systems which we must use to model this situation: the observer's coordinate system and the local coordinate system of the binary-star pairs. Let us define the observer's coordinate system such that its z-axis points directly from the binary towards the observer along the observer's line of sight. Let the x-axis coincide with the direction of $\boldsymbol{L}$ when $\psi = 0°$ and $i = 90°$. Using these definitions, a binary with an orbital angular momentum of $\boldsymbol{L} = (L_x, L_y, L_z)$
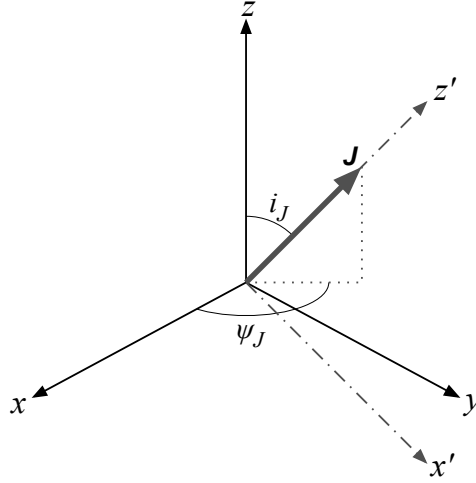
Figure 3.2: There are two coordinate systems that I use to describe spinning binary star systems. The observer coordinate system (solid lines) is defined such that its z-axis points directly away from the binary and towards the observer. Its x-axis is simply used as reference to calculate the angles ψ and ψ_J. The binary's local coordinate system (dashed lines) is defined such that its z axis coincides with its total angular momentum, while its x-axis points away from the observer's line of sight. Therefore, i_J is the angle between the z and z' axes, and ψ_J is the angle between the x-axis and the projection of z' onto the xy-plane.

will have an orientation of

$$i = \cos^{-1}\left(\frac{L_z}{|\boldsymbol{L}|}\right), \text{ and} \tag{3.7a}$$

$$\psi = \tan^{-1}\left(\frac{L_y}{L_x}\right). \tag{3.7b}$$

The observer's coordinate system makes it easy to calculate i and ψ, but very difficult to calculate the binary's precession. For that, we need to use the local coordinate system. Recall that the local coordinates that I have been using are defined such that the z-axis coincides with the total angular momentum, and that the x-axis points *away* from the line of sight. Its y-axis is defined such that the coordinate system is orthogonal and right-handed. Since the total angular momentum is constant, this coordinate system never changes. Figure 3.2 graphically shows the relationship between the two systems. One can transform from the local coordinate system to

the observer's coordinate system with the following matrix equation:

$$(3.8) \qquad \begin{bmatrix} L_x \\ L_y \\ L_z \end{bmatrix} = \begin{bmatrix} \cos\psi_J & -\sin\psi_J & 0 \\ \sin\psi_J & \cos\psi_J & 0 \\ 0 & 0 & 1 \end{bmatrix} \begin{bmatrix} \cos i_J & 0 & \sin i_J \\ 0 & 1 & 0 \\ -\sin i_J & 0 & \cos i_J \end{bmatrix} \begin{bmatrix} L'_x \\ L'_y \\ L'_z \end{bmatrix},$$

where the prime denotes the local reference frame. Equations 3.7a and 3.8 together show how the variables i and ψ change as the orbital angular momentum precesses in its local coordinate system.

In order to change the program so that it models spinning binary systems, I needed to modify all five of its basic tasks. Modifying the input and the output was trivial. I simply needed to change the user interface to include the six extra spin parameters, add six more variables to the code, and change the output to print uncertainty of the additional parameters. Note that the input orientation of the binary is now in reference to the orientation of its total angular momentum $\boldsymbol{J}$ instead of its orbital angular momentum $\boldsymbol{L}$. The corresponding input parameters are i_J and ψ_J instead of i and ψ. The final calculation of uncertainty was also fairly simple. I just needed to modify the inversion process so that it inverted a 15×15 matrix (for the 15 parameters) instead of a 9×9 matrix. Modifying the setup and the calculation of derivatives, on the other hand, was a complicated and involved process.

The first step in modifying the setup was to initialize the precession of the binary. To do this, I created a precessional object[4] that contains the core Runge-Kutta code that I used in the precessional simulations (see chapter 2.4). A single instance of the object contains all of the information needed to precess the binary in its local reference frame. I instantiated 10 precessional objects in the setup. The first instance models the binary system exactly as input by the user. The remaining nine objects model binary systems that differ from the first in one of the three orbital or six spin parameters. These are needed to calculate derivatives, as shown below.

The next step was to find all of the old constants that depended on either i or ψ, and turn them into variables. I did this by moving the old code into the main computational loop of the program. This causes the constants to be reevaluated at each time-step so that they change as the orbit precesses. Finally, I needed to add several new global variables to the setup. Most importantly, I needed to expand the information matrix to include all 15 parameters, and I needed to ensure that there were different variables to describe the orientations of $\boldsymbol{J}$ and $\boldsymbol{L}$. After this, changes to the setup were complete.

---

[4]An object is a type of structure in object-oriented programming languages that contains both instructions and data. In order to use an object it needs to be instantiated. Each instance will contain its own set of data that is independent from all other instances, as well as a common set of instructions that will act upon its own data.

Changing the computational loop of the program required three additions to the code. First, I needed to advance each of the precessional instances by one time-step. Second, I needed to recalculate all of the old constants, including the orientation angles i and ψ. These can be calculated directly from equations 3.7a and 3.8. Finally, I needed to recalculate the derivatives and input them into the information matrix. This last step requires some explanation.

The gravitational radiation received by LISA does not directly depend upon the spin parameters of the binary[5]. However, it does depend upon the orientation of the binary, and the orientation depends upon the spin and orbital parameters. Therefore, each of these parameters affects the gravitational radiation, and their derivatives needed to be calculated for the information matrix. Let the amplitude of a received gravitational wave be expressed as function of the 15 different input parameters q:

$$(3.9) \qquad\qquad h(t) = f(q_1, q_2, \ldots, q_{15}).$$

Note that the input parameters include the orientation of the total angular momentum i_J and ψ_J, but not the orientation of the orbital angular momentum i and ψ. The derivative of the received amplitude with respect to a single parameter q_a can then be written as

$$(3.10) \qquad\qquad \frac{\partial h}{\partial q_a} = \left(\frac{\partial h}{\partial q_a} \right)_{i,\psi} + \frac{\partial h}{\partial i} \frac{\partial i}{\partial q_a} + \frac{\partial h}{\partial \psi} \frac{\partial \psi}{\partial q_a},$$

where the subscript on the first term indicates that we are explicitly holding i and ψ constant. Note that the first term of this equation is equal to the old derivative without spin. This is equal to zero for the new spin and orientation parameters. The second and third terms contain factors of $\frac{\partial h}{\partial i}$ and $\frac{\partial h}{\partial \psi}$, neither of which changed by adding spin to the model. The only thing that is left to calculate is $\frac{\partial i}{\partial q_a}$ and $\frac{\partial \psi}{\partial q_a}$.

One can show that the derivatives of the orientation parameters can be expressed as a function of the orbital angular momentum in the observer's coordinate system:

$$(3.11a) \qquad \frac{\partial \psi}{\partial q_a} = \frac{1}{|\boldsymbol{L}| \sin i} \left(\cos \psi \frac{\partial L_y}{\partial q_a} - \sin \psi \frac{\partial L_x}{\partial q_a} \right), \text{ and}$$

$$(3.11b) \qquad \frac{\partial i}{\partial q_a} = \frac{1}{|\boldsymbol{L}|} \left[\cos i \left(\cos \psi \frac{\partial L_x}{\partial q_a} + \sin \psi \frac{\partial L_y}{\partial q_a} \right) - \sin i \frac{\partial L_z}{\partial q_a} \right].$$

The angular orbital momentum $\boldsymbol{L}$ and the angles i and ψ are known values that change with time. However, the derivatives of $\boldsymbol{L}$ are as of yet unknown. If $q_a = i_J$

---

[5]Strictly speaking, very large spinning objects do emit gravitational radiation. However, this radiation is very small compared to the radiation emitted by the orbital motion of a binary system (Kidder, 1995).

or $q_a = \psi_J$, then these derivatives can be calculated analytically. By taking the derivative of equation 3.8, one can show that

$$(3.12\mathrm{a}) \quad \frac{\partial L_x}{\partial \psi_J} = -L_y \qquad \frac{\partial L_y}{\partial \psi_J} = L_x \qquad \frac{\partial L_z}{\partial \psi_J} = 0, \text{ and}$$

$$(3.12\mathrm{b}) \quad \frac{\partial L_x}{\partial i_J} = (\cos \psi_J) L_z \qquad \frac{\partial L_y}{\partial i_J} = (\sin \psi_J) L_z \qquad \frac{\partial L_z}{\partial i_J} = -\left[(\cos i_J) L'_x + \sin i_J) L'_z\right].$$

We can substitute these derivatives into equations 3.10 and 3.11 to find expressions for $\frac{\partial h}{\partial i_J}$ and $\frac{\partial h}{\partial \psi_J}$. These can then be put directly into the information matrix via equation 3.5.

If q_a is anything else, then the derivatives on the right sides of equations 3.12 must be solved numerically. We can approximate the derivatives as

$$(3.13) \qquad\qquad \frac{\partial \boldsymbol{L}}{\partial q_a} \approx \frac{\boldsymbol{L}(q_a + \Delta q_a) - \boldsymbol{L}(q_a)}{\Delta q_a},$$

where q_a is the parameter as input by the user, and Δq_a is a small change in the parameter. In order to order to calculate this expression, I needed to compute both $\boldsymbol{L}(q_a + \Delta q_a)$ and $\boldsymbol{L}(q_a)$ at each time-step and for every parameter that affects the precession. This is why I needed to instantiate 10 precessional objects. Note that equation 3.13 actually calculates the derivatives at $q_a + \frac{1}{2}\Delta q_a$ instead of at q_a. This small error can be minimized by picking a suitably small Δq_a[6]. By substituting it into equations 3.10 and 3.11, this numerical computation finishes the calculation of $\frac{\partial h}{\partial q_a}$ and completes the information matrix.

Now, with all of the derivatives calculated, the program is complete and ready to find uncertainties. However, before closing this chapter I would like to point out a potential problem in the calculations. As noted in section 1, the initial phase ϕ_0 depends on the orientation of the binary, specifically on the angle ψ. Since ψ is no longer constant, there may be an error in the calculated phase of the gravitational radiation. If the precessional frequency is very low, as is our assumption, then this error is bound to be small. Although of minor physical importance, the problem itself is conceptually difficult, so, for completeness, I discuss it in some detail in Appendix B.

---

[6]It would be easy to calculate a centered difference derivative $\frac{\partial \boldsymbol{L}}{\partial q_a} \approx \frac{\boldsymbol{L}(q_a + \Delta q_a) - \boldsymbol{L}(q_a - \Delta q_a)}{2\Delta q_a}$, and not worry about the small error of the non-centered difference. The problem with this is that the program would require an additional instance of $\boldsymbol{L}(q_a - \Delta q_a)$ for every q_a that affects the precession, and it would need to evolve each of these extra instances each time-step. This significantly slows the program.

CHAPTER 4

Results

In this chapter, I use the program described in chapter 3 to find the uncertainties associated with measuring gravitational waves that come from spinning binary stars. The parameter space for this problem is enormous—with 15 input parameters, there are billions of different cases that one can study. For simplicity, I will focus on just one. I will examine how variations in its input parameters change its uncertainties, and compare these to a similar case with no spin.

An ideal case must meet several criteria. First, its orbital frequency must be large compared to its precessional frequency. This allows us to safely use the assumptions made in chapter 2.3. Second, the spin angular momentum needs to be large enough so that its effects are easily visible. Third, the resulting waveform needs to have a high signal to noise when measured by LISA. Lastly, the ideal case should be a physically reasonable system. To satisfy these criteria, I chose the following parameters: the mass of the first object is $m_1 = 1500 \, \mathrm{M_\odot}$ (solar masses); the second mass is $m_2 = 1000 \, \mathrm{M_\odot}$; $t_c = 20$ years; and $r = 50$ million light years. I modeled both masses as maximally spinning black holes ($\chi_1 = \chi_2 = 1.0$), with their spins oriented perpendicular to the total angular momentum and each other ($\theta_1 = \theta_2 = 90°$, $\phi_1 = 0°$, and $\phi_2 = 90°$). I treated the magnitudes of the spins as known parameters so that their derivatives did not enter the information matrix. These values produce a system with an orbital frequency of $\sim 1 \, \mathrm{mHz}$ and a measured gravitational wave amplitude of $\sim 2 \times 10^{-21}$. LISA should be very sensitive at this frequency, and have no trouble detecting such a wave. The precessional frequency of the system is only $\sim 0.6 \, \mu\mathrm{Hz}$, well below the orbital frequency (it completes 20 precessions in the course of a year), and the orbital angular momentum is inclined $\sim 4°$ away from the total angular momentum. The effect of this precession is much smaller than that of the case studied in chapter 2.4, but large enough to be detectable.

The r parameter places the system within the local super cluster of galaxies, and the masses might correspond to central black holes in dwarf galaxies. Thus, the system represents a nearby merger of central dwarf galaxy black holes. The chances that this situation could occur in any given year is small, but the situation itself is not completely physically implausible. If I were to model the precession more accurately and ignore the requirement that the precessional frequency be small, then
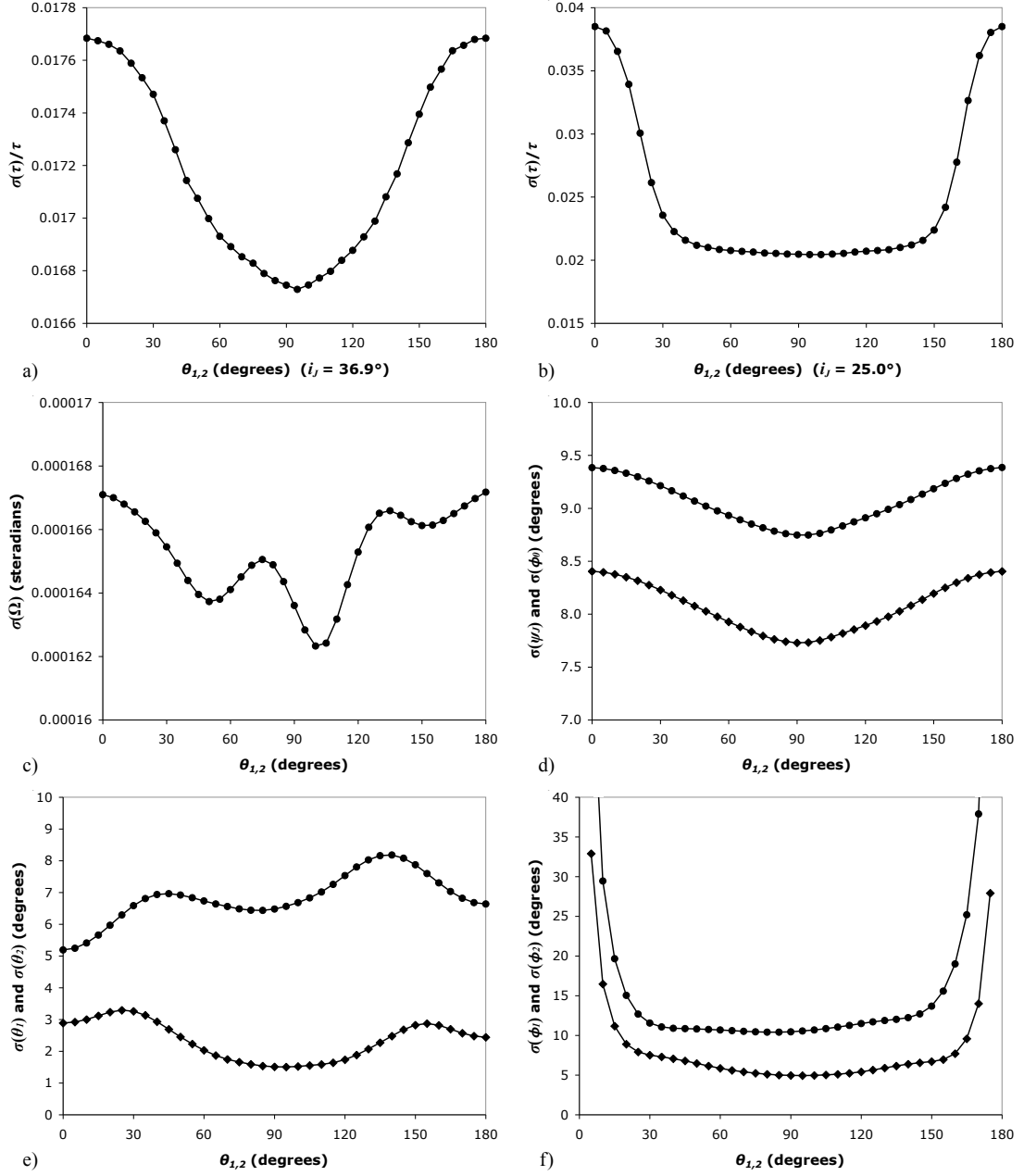
27

Figure 4.1: a) and b) Fractional uncertainty of τ at different spin angles $\theta_{1,2}$. In a), the inclination is at its default value of $i_J = 36.9°$. In b), it is at $i_J = 25.0°$. c) Positional uncertainty Ω of the binary system. d) Uncertainty of the parameters ψ (circles) and ϕ_0 (diamonds). e) Uncertainty of the spin parameters θ_1 (diamonds) and θ_2 (circles). f) Uncertainty of the spin parameters ϕ_1 (diamonds) and ϕ_2 (circles).

I would be able to find more common scenarios. However, the results of the present case should be qualitatively similar to the more common cases, so my conclusions will be fairly general.

The remaining parameters of the system have somewhat arbitrary values. I set these to be $i = 36.9°$ ($\cos i = 0.8$), $\psi = 30.0°$, $\phi_0 = 0.0°$, $\Theta = 5.0°$, and $\Phi = 268.5°$. With the exception of ψ, these were the default values used by Moore and Hellings (2002). I set the program to sample the gravitational waveform once every 200 seconds, or approximately 5 times per orbital period. Higher sampling rates did not significantly affect the calculated uncertainties.

In the following sections, I will vary some of the input parameters and describe the resulting uncertainties. I vary θ_1 and θ_2 in section 1, the inclination i_J in section 2, and ψ_J in section 3. In each case, all of the other parameters remain at their original values.

1. Variations in θ_1 and θ_2

The first thing that I examined is the effect of the spin angles θ_1 and θ_2 upon the calculated uncertainties. These angles directly determine the angle between the orbital angular momentum $\boldsymbol{L}$ and the total angular momentum $\boldsymbol{J}$, and thereby determine the magnitude of the precession. When the spin angular momenta are either aligned or anti-aligned with the total angular momentum ($\theta_{1,2} = 0°$ or $180°$, respectively) $\boldsymbol{L}$ becomes parallel to $\boldsymbol{J}$ and there is no precession. When the spins are perpendicular to the total angular momentum, the angle between $\boldsymbol{L}$ and $\boldsymbol{J}$ is at a maximum and the precession is large. Therefore, we expect the effect of the spins upon the uncertainties to be non-existent at $\theta_{1,2} = 0°$ and $180°$, and near its peak at $\theta_{1,2} = 90°$. Note that the effect is not symmetric about $\theta_{1,2} = 90°$. This is because $\boldsymbol{J}$ is largest when it is aligned with the spins, and smallest when it is anti-aligned with them.

Figure 4.1 shows how some of the uncertainties change as the spin angles increase. Of the 14 calculated uncertainties[1], there were 6 groups of parameters with similar qualitative features. The first two graphs, figures 4.1a and 4.1b, show how the uncertainty of the mass variable τ changes with spin angle. The uncertainties in parameters r and i_J have roughly the same functional shape as τ, while the uncertainty in δ is almost exactly 4 times the fractional uncertainty of τ. The graph of the solid angle uncertainty of the binary's position (figure 4.1c) is qualitatively similar to the uncertainties of t_c, Θ, and Φ, none of which significantly change with spin.

----

[1]There are 15 input parameters with associated uncertainties, but I have set χ_1 and χ_2 as constants. The final uncertainty is $\sigma(\Omega)$, the uncertainty of the object's position measured in steradians.
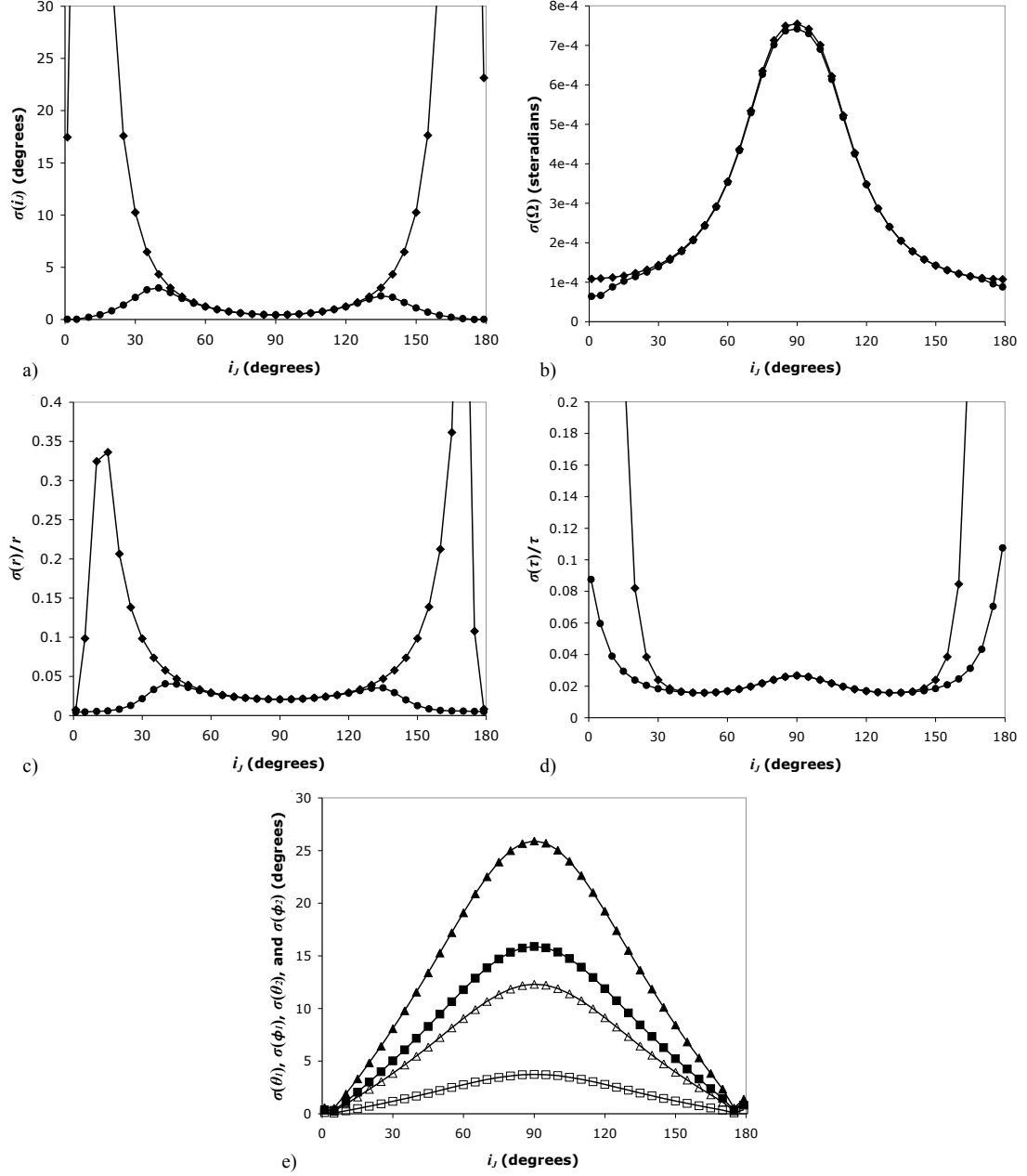
Figure 4.2: Uncertainties in binary parameters with changing inclination i_J. In all cases, circles represent the uncertainties of the binary system modeled with spin, and diamonds represent the uncertainties of the system without spin. a) Uncertainty of the inclination angle i_J. Note that $\sigma(i_J)$ goes to zero as i_J approaches either 0° or 180° for both spinning and non-spinning binaries. b) Positional uncertainty Ω of the binary systems. c) Fractional uncertainty of r. d) Fractional uncertainty of τ. e) Uncertainty of the spin parameters (for spinning binaries only). The uncertainties of θ_1, θ_2, ϕ_1, and ϕ_2 are represented by hollow squares, hollow triangles, solid squares, and solid triangles, respectively.

The uncertainty of ψ closely resembles the uncertainty of ϕ_0 (figure 4.1d), and the uncertainties of the two spin angles (figures 4.1e and 4.1f) have very similar forms.

There are two very interesting results that can be gleaned from these graphs. First, the binary's precession has very little effect upon the positional uncertainty. If this uncertainty was already high, then there is little hope that the presence of spin will enable LISA to locate binary systems with enough accuracy to be observed with conventional telescopes. Second, the presence of spin can have a very large effect upon the uncertainty of the total mass τ and the radius r, and this effect is larger at smaller inclination angles. These two uncertainties are closely related since, to first order, they only affect the amplitudes of received gravitational waves. By reducing the mass uncertainty, one can gain a greater understanding of the binary system itself and thereby gain understanding of its local environment. And, by reducing the radial uncertainty, one *might* be able to find a host galaxy with a matching a radial coordinate.

2. Variations in i_J

The inclination i_J of the binary ought to have a very large effect upon the calculated uncertainties. The inclination of the orbital angular momentum i, the mass difference δ, and the phase ϕ are the only variables that determine the post-Newtonian corrections[2] to the amplitude of the gravitational wave. At $\sin i = 0$, the first order corrections to the waveform disappear, and at $\cos i = 0$, the zeroth order cross polarization disappears (Blanchet et al., 1996). Since i changes in precessing binary systems, the addition of spin will greatly change the way in which i_J affects the uncertainties.

Figure 4.2 shows some of the more interesting changes that occur with varying i_J. In all of the graphs, circles represent uncertainties for binaries with spin and triangles represent uncertainties for binaries without spin. First, the uncertainty of the inclination changes by a large amount (figure 4.2a). The uncertainty is low at $i_J = 0°$, $90°$, and $180°$, and high elsewhere. Presumably, this is because parts of the waveform vanish at these angles, so that a small change in i_J creates a large change in the received gravitational wave. By including spin, we can reduce this uncertainty by as much as a factor of 100. The same cannot be said of the positional uncertainty Ω, which barely changes at all when we add spin (figure 4.2b). The positional certainty of the binary mainly depends upon the Doppler effect measured by LISA as it orbits the sun, so only the zeroth order terms of the gravitational wave have a great effect.

---

[2]A post-Newtonian correction is a correction that takes into account the general relativistic non-Keplerian orbits of binary pairs. The zeroth order correction of the gravitational wave amplitude is of the order $\epsilon^2 = \left(\frac{\tau\omega}{5}\right)^{2/3}$, where ω is the angular frequency of the orbit in the binary's local frame. Each subsequent correction has an additional coefficient of ϵ.
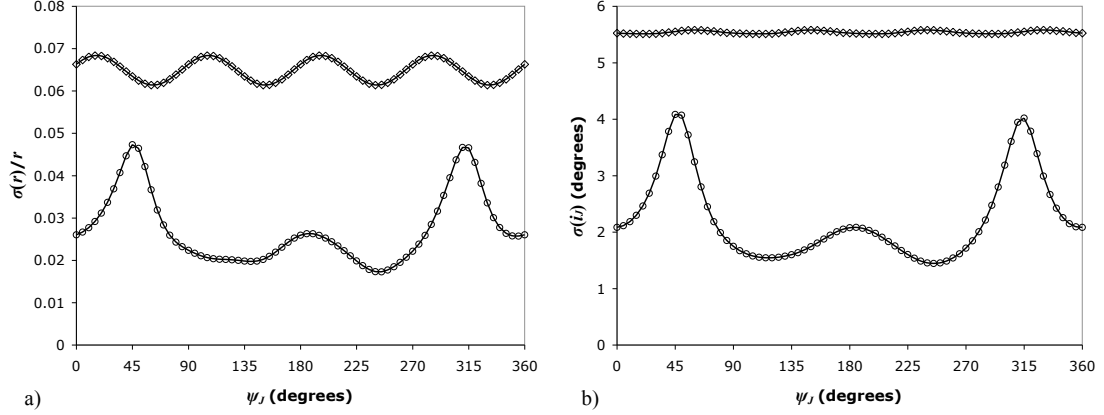
Figure 4.3: Uncertainties in binary parameters with changing orientation ψ_J. In both cases, circles represent the uncertainties of the binary system modeled with spin, and diamonds represent the uncertainties of the system without spin. a) Fractional uncertainty of r. b) Uncertainty of the inclination angle i_J.

These terms peak at $i_J = 0°$ and $180°$, while the positional uncertainty peaks at $i_J = 90°$ and is at minima at $i_J = 0°$ and $180°$, as expected.

Both the uncertainty in the radial coordinate (figure 4.2c) and total mass (figure 4.2d) are greatly reduced by the addition of spin. Note that the uncertainty in δ (not shown) is always 4 times the fractional uncertainty of τ. Spin increases the radial accuracy by as much as a factor of 65, and it can increase the accuracy of the mass by a factor of 15. These benefits are most prominent when $\sin i_J$ approaches zero. At these locations, the precession and the variability of i provide large amounts of information. At $\sin i_J \approx 90°$, changes in i produce negligible changes in $\sin i$, and the benefit of precession is very small. The nature of this benefit may also be due to the fact that the angle ψ is undefined at $\sin i = 0°$, and this decreases the amount of available information. The additional information provided by the precession then has a greater effect near these angles.

The uncertainty of the spin orientations is greatest at $i_J = 90°$, and lowest at $i_J = 0°$ and $180°$ (figure 4.2e). The presence of spin is most important at low inclinations, so at these angles we expect to find a large amount of information about the spin itself. As seen in the graph, one can calculate the spin orientations with an uncertainty of less than $1.0°$ near $i_J \approx 5°$, and, at $i_J \approx 90°$, the uncertainty drops by a factor of 50.

3. Variations in ψ_J

In general, variations in the angle ψ_J have very little effect upon the calculated uncertainties. Figure 4.3 shows how they affect the uncertainties in r and i_J. Its effect upon all of the other uncertainties is negligible. Without spin, the changes in uncertainty caused by different ψ_J are easy to understand. By rotating the orientation of the binary (and ψ_J) by 45°, one changes the plus polarizations of the received gravitational wave into cross polarizations. Another 45° rotation changes the cross polarizations back to plus polarizations, but puts them 180° out of phase. Of course, after half an orbital period the phase will return to its original value, so there should be a repeating pattern in the uncertainties every 90° of ψ_J. One can clearly see this pattern in binaries without spin.

A very different pattern occurs when we add spin to the model. The uncertainties no longer repeat every 90° of ψ_J. Instead, the uncertainty is roughly symmetric about $\psi_J = 180°$. This contrasts with the behavior of binaries without spin, in which the uncertainty is exactly anti-symmetric about $\psi_J = 180°$. The variability of the uncertainty is also much greater in the cases with spin. It increases by a factor of ~ 3 for the uncertainty of r, and by a factor of ~ 30 for the uncertainty of i_J. These counterintuitive results have no simple physical explanation. One can only conclude that the presence of spin changes the way the in which ψ_J affects the uncertainties, and, in the cases of the r and i_J parameters, this change can produce significantly different results.

4. Variations in other parameters

The input parameter space for these simulations is incredibly large, and I have just barely scratched the surface of the possible scenarios that one might compute. However, we can make some intelligent guesses as to how variations in other parameters will affect the uncertainty.

Several of the parameters ought to have very little effect upon the uncertainty, regardless of the presence of spin. If the binary is far from coalescence, then there is no preferred direction for the positional angle Φ and its value will have little effect. The initial phase ϕ_0 makes no difference in the uncertainties because the phase changes with time and continuously varies from 0° to 360°. Thus there is no preferred initial phase. Similarly, the initial spin angles ϕ_1 and ϕ_2 do not matter because they continuously vary from 0° to 360° with different frequencies[3].

Other parameters should have predictable effects. An increase in τ or a decrease in t_c would cause both the amplitude of the gravitational wave and the magnitude of

---

[3]If the two spinning objects have approximately the same mass, then the spin angles will vary with the same frequency and the angle between them will be nearly constant. In this case, the angles ϕ_1 and ϕ_2 should create substantive changes in the uncertainties.

the precession to increase. This would cause an overall reduction in uncertainty and increase the importance of the spins. An increase in $|\delta|$ would have just the opposite effect. An increase in the radial coordinate r would only make the wave amplitude and signal-to-noise decrease, and cause an overall increase in the uncertainty. It would not change the precession, but the relative importance of the spin may increase as the signal decreases.

The only parameter that might cause unpredictable results is the positional angle Θ. As shown by Moore and Hellings (2002), variations in Θ can cause several different effects, depending upon the orbital parameters of the binary. I suspect that the addition of spin would decrease the uncertainties most when Θ tends to increase them, much like the way it decreases the uncertainties in figures 4.2c and 4.2d. However, this hypothesis would need verification.

CHAPTER 5

Conclusion

In the preceding chapters, I have described the way in which the space-based gravitational wave observatory LISA can measure the orbital parameters of binary stars, and how the spins of the stars can affect these measurements. There are several important results to draw from these discussions. First, the presence of spin can have a very large effect upon the orbital motion of the stars, and this motion is not easily calculable. Without spin, stars orbit circularly and slowly spiral inwards as they lose angular momentum and energy with released gravitational radiation. With spin, the orbital plane of the stars precesses about the system's total angular momentum while the stars continue in their circular orbits, and this precession can exhibit complicated 'spirograph' behavior. Second, ignoring the small contribution that the spinning stars directly make to the gravitational wave, the only way that one can detect the presence of spin is to measure the precession of the binary's orbital plane. This precession can be seen as a change in the orientation of the binary system, and this change can be measured by LISA. Last, the presence of spin causes potentially large increases in the certainty with which LISA can measure orbital parameters. This is particularly true when the binary is viewed nearly face-on, where the accuracy in the mass parameters can increase by a factor of 15, and the accuracy in the distance to the system can increase by a factor of 65. Such increases in accuracy would be immensely useful in scientific analysis. A better measurement of the mass of a binary would allow one to gain a greater understanding of the binary system itself and the environment in which it resides, and a better measurement of the distance to the binary might allow one to localize it to a particular galaxy, which could then be studied with conventional optical telescopes.

There is a large amount of work in this subject that still needs to be done. As stated in chapter 2, I have used a simplified version of the precessional equations of motion, one which is not valid in a large number of physically interesting cases. How does the inclusion of spin in these cases affect the uncertainty of orbital parameters as measured by LISA? Will these cases show similar increases in accuracy to the case discussed above? Or will there be higher-order effects that change the uncertainties in unpredictable ways? Only further research can answer these questions.

Also, I have only examined a tiny fraction of the number of available cases, even excluding those for which the simplified precessional equations are invalid. By examining a larger variety of simulations, one might be able to find interesting patterns with interesting physical explanations. These explanations could then be used to describe some of the unpredicted results found in chapter 4.

Astronomers are on the verge of an observational breakthrough. They will soon have access to new signals from the stars in the form of gravitational radiation. The results presented here show some of the vast potential that this exciting breakthrough will have.

Motivating Gravitomagnetism

The phenomenon of gravitomagnetism can be derived directly from Einstein's equations of general relativity. However, this derivation is far from obvious, and it is beyond the scope of this thesis to explain it here. Instead, I will motivate gravitomagnetism by explaining how it works in a particular scenario. To begin this discussion, I will need to describe the basics of metrics and curved space-time.

A metric is a way of relating changes in coordinate position to physical changes in spatial and temporal displacement. For flat Euclidean space-time, also known as Minkowskian space-time, the metric equation is

$$(A.1) \qquad\qquad ds^2 = -dt^2 + dx^2 + dy^2 + dz^2.$$

This equation relates the space-time interval, ds, to the changes in spatial and temporal coordinates between two events. Note that we are using a system where time and distance have identical units, and where the speed of light is equal to one[1]. If no time has elapsed, then equation A.1 just reduces to the Pythagorean Theorem, as one would expect for normal space. It is useful to define the proper time between two nearby events as $d\tau^2 \equiv -ds^2$. The proper time is the time measured by an observer that travels from one event to another. If there is no spatial difference between the two events, then equation A.1 says that the proper time is simply the change in coordinate time (dt). If the two events are separated both spatially and temporally, then the proper time will be less than the change in coordinate time. This is because an observer will have to move quickly to get from one event to the other, so relativistic time dilation will occur and the observer's clock will appear to tick more slowly.

So far, the discussion of metrics has only involved special relativity, where space-time is flat. In general relativity this is not always the case. One of the basic concepts of general relativity is that massive objects bend space-time, and therefore they change the metric equation. For this discussion we are interested in the metric surrounding rotating massive objects. Arguments from symmetry will give us a good idea of what this metric should look like. First, let us write down the metric for flat,

---

[1] If we choose to work in units of distance, then one meter of time is the time that it takes for light to travel a meter. Likewise, if we work in units of time, then one second of distance is the distance that light travels in one second.

spherically symmetric space:

$$ds^2 = -dt^2 + dr^2 + r^2 d\theta^2 + r^2 \sin^2 \theta d\phi^2 \tag{A.2}$$

This equation uses spherical polar coordinates, where r is the radial coordinate, θ is the azimuth angle, and ϕ is the latitudinal angle. Note that the coefficient to the time part of the metric remains unchanged, and that $d\theta$ and $d\phi$ both have non-constant coefficients. We know that the metric outside of any massive body must reduce to equation A.2 far away from the system's center. That is, space-time must be flat far away from massive objects. Therefore, a reasonable first guess for the metric outside of a rotating object is

$$ds^2 = g_{tt}dt^2 + g_{rr}dr^2 + g_{\theta\theta}d\theta^2 + g_{\phi\phi}d\phi^2 \tag{A.3}$$

where the different g's are potentially complicated coefficients that reduce to the coefficients in equation A.2 at large r. However, it is also possible to have cross product terms such as $g_{r\theta}drd\theta$. What would such a term mean? In this case, it would signify that one travels a different distance when moving outwards and up then when one moves outwards and down, since $d\theta$ will have a different sign. This particular term is physically unreasonable, since there should not be anything special about moving up instead of down or out instead of in. Only the ϕ coordinate could have such odd antisymmetry, since our hypothesized massive object is rotating in a particular ϕ-direction. Therefore, we expect that the metric will have a term of the form $g_{t\phi}dt\,d\phi$. This means that one travels further when going clockwise about the system's center (for example) than when one is going counterclockwise. If one very carefully does all of the calculations, one can find that the metric on the equatorial plane ($\theta = 90°$) outside of a spinning object is

$$
\begin{aligned}
ds^2 = &- \left(1 - \frac{2GM}{r}\right)dt^2 + \left(1 - \frac{2GM}{r} + \frac{a^2}{r^2}\right)^{-1} dr^2 + r^2 d\theta^2 \\
&+ \left(r^2 + a^2 + \frac{2GMa^2}{r}\right)d\phi^2 - \frac{4GMa}{r}d\phi dt,
\end{aligned}
\tag{A.4}
$$

where G is the gravitational constant, M is the object's mass, and a is a parameter that is related to how fast the object spins. This is known as the Kerr metric (Kerr, 1963). Granted, this equation is very complicated (and it is even more complicated off of the equatorial plane), but there are only a few features which we need to pay attention to in order to understand gravitomagnetism. Most importantly, there is a term involving $dtd\phi$ that becomes small at large radii, and its magnitude and sign depend on how fast and in what direction the object is spinning.

With the Kerr metric, we have almost everything we need to explain gravitomagnetism. However, we still do not understand how objects move in Kerr space-time. In general, freely floating objects travel in the straightest possible lines. However,
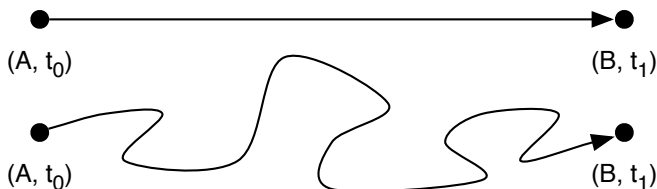
Figure A.1: Bob needs to get from point A at time a t_0 to point B at a time t_1. The shortest path that he can take is the straight line from A to B. If he takes a more circuitous route, then he must travel faster to reach point B in the same amount of time. As he travels faster, the relativistic time-dilation effects increase and his proper time decreases. The shortest path minimizes this effect.

straight lines in curved space-time are no longer straight, so we need a more useful description. An object traveling in a straight line between two points in space-time will experience the *largest* possible proper time between those two points. That is, a freely floating object will always travel in a path that maximizes its proper time. This is most easily illustrated in flat space-time, but it applies equally well to any curved space-time. Suppose that a person (let's call him Bob) tries to move from some point A at a time t_1 to another point B at a time t_2. If Bob takes a very circuitous route instead of a short straight route, then he must travel very fast in order to cover a larger distance in the same allotted amount of time (see figure A.1). He will experience time dilation effects, and his clock will tick slowly. If instead Bob takes a direct route, he will not have to travel as fast and his clock will tick more quickly. Therefore, Bob's straight-line route is the route that gives him the longest proper time.

Now, suppose that Bob lives in Kerr space-time and that he is trying to get closer to the system's center. What is his straightest route? Figure A.2 shows two possible routes that he could take. In figure A.2a Bob travels straight towards the system's center, whereas in A.2b he curves slightly to his right. The space-time interval for the straight path is going to be given purely by the dt^2 and dr^2 components of the metric. The curved path will have approximately the same radial and time components, but it will also have a $d\phi^2$ and a $dtd\phi$ component. Although the $d\phi^2$ component acts to increase ds^2, the $dtd\phi$ component actually decreases ds^2, and thereby *increases* the proper time. This can be seen as follows. When Bob starts on the curved path he is moving clockwise against the spin of central mass. Since he moves in the $-\phi$ direction and since the $dtd\phi$ coefficient is negative, this move creates a positive contribution to ds^2. When he reaches the halfway point on the path he starts to go counterclockwise, creating a negative contribution to ds^2. However, as Bob gets closer to the center his radius decreases and the absolute value of the $dtd\phi$ coefficient (which is proportional to $1/r$) increases. Therefore, the negative contribution of the
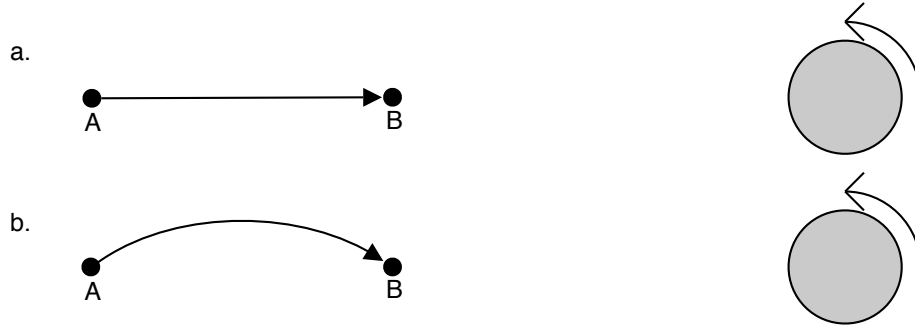
Figure A.2: In (a), Bob appears to travel in a straight line toward the system's center. He moves only $-r$ direction. In (b), Bob travels in a curved path, but he takes the same amount of coordinate time to reach point B. The curved path moves in both the $\pm\phi$ and the $-r$ directions. It turns out that if the curve is small enough, Bob's clock will tick faster on the curved route then on the apparently straight route. That is, Bob's proper time is maximized on the curved path, so it is actually the straightest line between points A and B in this curved space-time.

counterclockwise motion outweighs the positive contribution of the clockwise motion. For some reasonably small curved path, this net negative contribution is greater than the positive contribution of the $d\phi^2$ component, so $\Delta\tau = \int d\tau$ is maximized. Bob's straightest route actually curves to his right!

By running through similar arguments in different scenarios, one finds that the rotation of the system's central massive object always causes Bob's path to curve slightly to the right of where it would otherwise go. It is as if there is a fictitious force that pushes Bob perpendicular to his direction of motion. Let us image that there is a gravitomagnetic field created by the spinning mass. This field is completely analogous to a magnetic field created by a spinning ball of charge. For a counterclockwise spinning mass, as viewed from the top, the field will point up out of the mass's north pole and down into the equatorial plane. We can then characterize the fictitious force as

$$(A.5) \qquad\qquad \boldsymbol{F}_{gm} \propto -m\boldsymbol{v} \times \boldsymbol{G},$$

where m is the mass of the moving object (in this case, Bob), $\boldsymbol{v}$ is the object's vector velocity, and $\boldsymbol{G}$ is the gravitomagetic field. This is exactly analogous to the force that a magnetic field imposes upon a moving charge.

Even though this proof of gravitomagnetism is far from rigorous, the analogy itself is actually quite robust. The gravitomagnetic analogy to Maxwell's equations of electromagnetism (equations 2.3) can be derived directly from the weak-field limits of general relativity (Mashhoon et al., 2001), so the analogy works in any reasonably flat section of space.

APPENDIX B

The Phase Problem

The phase problem describes a difficulty in defining the phase of a binary system. In non-spinning binary systems, the phase is defined as the angle between one of the masses and the semi-major axis of the binary's orbit as viewed from earth (see figure 3.1). The orientation of the semi-major axis is, in turn, defined by the angle ψ. These definitions are somewhat arbitrary—we could have defined these angles in reference to anything else and the physics of situation would not have changed. As long as one is consistent, the definitions do not matter.

In non-spinning systems all of the reference angles are constant, and we do not need to worry much about how the angles are defined. In spinning binary systems, the angle ψ is not constant, and we do need to worry. The question is, how does the movement of the angle ψ change the way in which we measure the phase ϕ?

Figure B.1 helps in understanding this question. Suppose that we are viewing a binary system with an orbital period of 1.0 second and a precessional period of 8.0 seconds. If the binary's total angular momentum points directly towards us, then the orbital angular momentum $\boldsymbol{L}$ will appear to sweep out a full circle every 8.0 seconds. That is, the angle ψ will increase by 360° every precessional period. After 1.0 second,
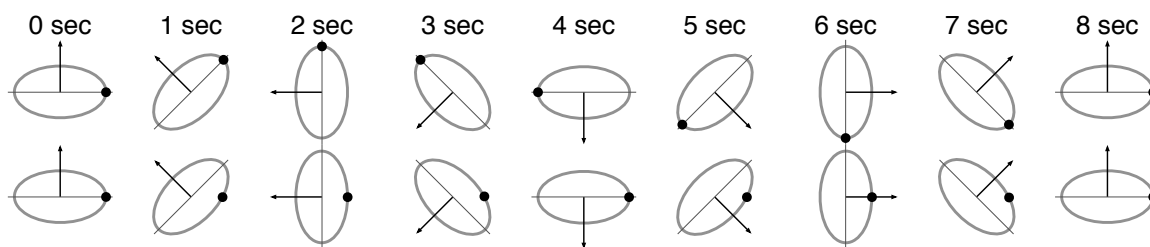

Figure B.1: Two different ways in which the phase of the orbit may change with precession. In each case, the binary has an orbital period of 1.0 second, and a precessional period of 8.0 seconds. The arrows represent the orbital angular momentum $\boldsymbol{L}$, while the total angular momentum points directly up out of the page. In the top row, the reference mass (solid dot) rotates 360° in the moving frame of the orbital plane every second. The orbital frame rotates 45° a second, so it appears that the reference mass rotates 405°. In the bottom row, the reference mass rotates 360° every second in the fixed frame of the observer.

ψ equals 45°, but what is the phase? A naive answer would be that the phase is right back where it started, at $\phi = 0°$. But since ψ has changed, this places the reference mass 45° away from its original location. After 8.0 seconds, the reference mass will *appear* to have completed one extra orbit, so that its *apparent* orbital period is only $^8\!/_9$ of a second.

The other possibility is that the position of the reference mass moves independently of ψ, so it really does end up in the same location after every second. This is what happens in the bottom sequence in figure B.1. If this is the case, then the apparent orbital momentum remains 1.0 second, but each second the phase is different. Using our original definition of ϕ, we can see that the phase must change like

(B.1) $$\phi(t) = \phi'(t) - \psi(t),$$

where $\phi'(t)$ is what the phase would be without precession. This would change the calculation of uncertainty in two distinct ways. First, every instance of ϕ that goes into the calculation of the gravitational wave h would need to be replaced with equation B.1. Second, there would be more ψ derivatives to go into the information matrix. Using equation B.1, we can write the ψ derivative of h as

(B.2) $$\frac{\partial h}{\partial \psi} = \left(\frac{\partial h}{\partial \psi}\right)_\phi + \left(\frac{\partial h}{\partial \phi}\right)_\psi \frac{\partial \phi}{\partial \psi}.$$

The first term is the just the old derivative, with the old definition of ϕ. Note that $\frac{\partial \phi}{\partial \psi} = -1$, and that a change in ϕ_0 has the same effect as a change in ϕ. Then we can rewrite equation B.3 as

(B.3) $$\frac{\partial h}{\partial \psi} = \left(\frac{\partial h}{\partial \psi}\right)_\phi - \left(\frac{\partial h}{\partial \phi_0}\right)_\psi.$$

We can plug this into equation 3.10 to get the new components of the information matrix.

It is unclear which of these two possibilities is correct. Luckily, for the regime in which we are interested, it does not matter. If the orbital period is much shorter than the precessional period, then the apparent orbital period will be almost identical for the two possibilities, and the effect upon the phase will be very small.

Bibliography

J. B. Hartle, *Gravity: An Introduction to Einstein's General Relativity* (Addison Wesley, 2002), 1st ed.

H. Karttunen, P. Kröger, H. Oja, M. Poutanen, and K. J. Donner, *Fundamental Astronomy* (Springer, 2003), 4th ed.

P. S. Shawhan, American Scientist **92** (2004).

K. Danzmann and A. Rüdiger, Classical and Quantum Gravity **20**, S1 (2003).

T. A. Moore and R. W. Hellings, Phys. Rev. D **65**, 062001 (2002).

L. Blanchet, B. R. Iyer, C. M. Will, and A. G. Wiseman, Classical and Quantum Gravity **13**, 575 (1996).

B. Mashhoon, F. Gronwald, and H. I. M. Lichtenegger, in *LNP Vol. 562: Gyros, Clocks, Interferometers: Testing Relativistic Gravity in Space*, edited by C. Lämmerzahl, C. W. F. Everitt, and F. W. Hehl (2001), p. 83.

L. E. Kidder, Phys. Rev. D **52**, 821 (1995).

R. P. Kerr, Phys. Rev. Lett. **11**, 237 (1963).